

Generation of a mean flow by an internal wave

B. Semin, G. Facchini, F. Pétrélis, and S. Fauve

Citation: [Physics of Fluids](#) **28**, 096601 (2016); doi: 10.1063/1.4962937

View online: <https://doi.org/10.1063/1.4962937>

View Table of Contents: <http://aip.scitation.org/toc/phf/28/9>

Published by the [American Institute of Physics](#)

Articles you may be interested in

[Experimental observation of a strong mean flow induced by internal gravity waves](#)

[Physics of Fluids](#) **24**, 086602 (2012); 10.1063/1.4745880

[Internal wave instability: Wave-wave versus wave-induced mean flow interactions](#)

[Physics of Fluids](#) **18**, 074107 (2006); 10.1063/1.2219102

[The mean flow and long waves induced by two-dimensional internal gravity wavepackets](#)

[Physics of Fluids](#) **26**, 106601 (2014); 10.1063/1.4899262

[Reflection of an internal gravity wave beam off a horizontal free-slip surface](#)

[Physics of Fluids](#) **25**, 036601 (2013); 10.1063/1.4795407

[The effects of near-bottom stratification on internal wave induced instabilities in the boundary layer](#)

[Physics of Fluids](#) **29**, 016602 (2017); 10.1063/1.4973502

[Selection of internal wave beam directions by a geometric constraint provided by topography](#)

[Physics of Fluids](#) **29**, 066602 (2017); 10.1063/1.4984245

PHYSICS TODAY

WHITEPAPERS

ADVANCED LIGHT CURE ADHESIVES

Take a closer look at what these environmentally friendly adhesive systems can do

READ NOW

PRESENTED BY
 MASTERBOND
ADHESIVES | SEALANTS | COATINGS

Generation of a mean flow by an internal wave

B. Semin, G. Facchini, F. Pétrélis, and S. Fauve

Laboratoire de Physique Statistique, École Normale Supérieure, PSL Research University, Université Paris Diderot Sorbonne Paris-Cité, Sorbonne Universités UPMC Univ Paris 06, CNRS, 24 Rue Lhomond, 75005 Paris, France

(Received 14 March 2016; accepted 1 September 2016; published online 22 September 2016)

We experimentally study the generation of a mean flow by a two-dimensional progressive internal gravity wave. Due to the viscous damping of the wave, a non-vanishing Reynolds stress gradient forces a mean flow. When the forcing amplitude is low, the wave amplitude is proportional to the forcing and the mean flow is quadratic in the forcing. When the forcing amplitude is large, the mean flow decreases the wave amplitude. This feedback saturates both the wave and the mean flow. The profiles of the mean flow and the wave are compared with a one-dimensional analytical model. Decreasing the forcing frequency leads to a wave and a mean flow localized on a smaller height, in agreement with the model. *Published by AIP Publishing.* [<http://dx.doi.org/10.1063/1.4962937>]

I. INTRODUCTION

A wave propagating through a fluid generally induces a mean flow. For example, acoustic waves generate a mean flow called “acoustic streaming,”^{1,2} sea waves approaching a coastline at an oblique angle induce a mean current parallel to the coastline,^{3,4} and internal gravity waves induce a mean wind in the equatorial Earth stratosphere.⁵

This article focuses on the mean flow induced by an internal gravity wave. This generation of a mean flow is an important issue in geophysics because this mean flow can induce material transport and promote mixing in the ocean.⁶ In planetary atmospheres, internal gravity waves can generate a coherent and strong wind. For example, in the equatorial Earth stratosphere, there is a wind which is inhomogeneous in height and which undergoes reversals with a period of approximately 28 months. This is known as the quasi-biennial oscillation.⁵ Similar winds are observed in Jupiter⁷ and in Saturn.⁸ In Venus, wave-mean flow interaction may explain the super-rotation phenomenon.⁹

A plane progressive homogeneous internal gravity wave does not induce any mean flow. To generate a mean flow it is thus necessary to consider an inhomogeneous wave. This inhomogeneity can be due to the transient character of the wave, for instance, if we consider a wave-packet.^{10,11} It can also be due to the dissipation of the wave.^{12,13}

Experimental studies of the generation of a mean flow by internal waves are scarce. King *et al.*⁶ have investigated the wave and mean flow generated by the tidal flow over a half-sphere. A strong mean flow in the direction perpendicular to the forcing has been measured. G. Bordes *et al.*¹⁴ have forced an internal wave using a vertical wave generator narrower than the channel. The inhomogeneity is due to the dissipation and to the localization of the wave (see also a numerical modelization in the work of Kataoka and Akylas¹⁵). A mean flow with a non-zero vertical vorticity is generated by the wave.

A different geometry has been investigated by Plumb and McEwan¹⁶ and Otake *et al.*,¹⁷ to provide an analog of the quasi-biennial oscillation. A stratified fluid is located between two concentric vertical cylinders and is forced by membranes located at the top or at the bottom of the fluid. Each membrane oscillates in opposition of phase with its 2 neighbors. The flow is mainly two-dimensional (2D). If the forcing amplitude is high enough, a mean flow is generated and oscillates with a period which is very long compared to the wave period.

We use a similar setup to study the generation of a mean flow by internal waves. In contrast to the experiments by King *et al.* and Bordes *et al.*, the flow is 2D due to the confinement by the walls. In contrast to the experiments by Plumb and McEwan and Otobe *et al.* where the wave is stationary in the azimuthal direction, the wave is progressive in the azimuthal direction in our experiments. The configuration is thus simpler which allows us to investigate both the linear and non-linear regimes and to compare the experimental data with an analytical model. We focus on the feedback of the mean flow on the wave, because it is an essential ingredient of the quasi-biennial oscillation. This feedback has not been experimentally investigated to the best of our knowledge.

In Sec. II, we present the experimental setup. The model is described in Sec. III. In Sec. IV, we present the results on the effect of the amplitude of the forcing on the wave and the mean flow. We then focus on two different amplitudes: one for which the feedback is negligible, and one for which it is large. Section IV D presents the influence of the wave frequency.

II. EXPERIMENTAL SETUP

A schematic view of the experimental setup is shown in Figure 1. It is made of two transparent concentric cylinders whose axes are along the vertical. This geometry is similar to the one in the work of Plumb and McEwan¹⁶ and Otobe *et al.*¹⁷ The outer diameter of the inner cylinder is 365 mm, the inner diameter of the outer cylinder is 600 mm, and the fluid height is 408 mm.

A linearly density-stratified fluid is injected between these two cylinders. This fluid is a solution of NaCl in water. The stratification is obtained using the classical double-bucket method.¹⁸ To ensure a smooth filling, the fluid is injected at the bottom through a porous medium. The conductivity is measured using a conductivity probe (Mettler-Toledo SevenGo Pro) positioned at different heights using a linear translation stage. The density profile and the Brunt–Väisälä frequency N are deduced from these measurements. This frequency is defined by $N^2 = (g/\rho_0) d\rho_0/dz$, where g is the acceleration of gravity, ρ_0 the background density, and where the axis z is defined in Figure 1. The typical value of this frequency is 1.5 rad s^{-1} . The dynamic viscosity η_e is deduced from the temperature and density measurements using tables¹⁹ and is close to the one of pure water.

The fluid motion is forced using 16 silicone membranes which are in contact with the top of the fluid. Each membrane can be individually moved up and down by a stepper motor (Nanotec L2818-OV15601 with SMCI36 controller). The membrane is fixed to the motor stick using two plates (typical dimensions $45 \times 45 \text{ mm}$) and screws. In this article, the forcing is a sine function for each motor, and the phase difference between two successive motors is $\pi/2$. This leads to a forcing whose azimuthal wavelength $\lambda_x = 400 \text{ mm}$ is the curvilinear distance between 4 motors.

To avoid a weakening of the stratification due to the mixing induced by the forcing, stratified fluid is continuously injected at the bottom and sucked at the top (Reglo ICC Ismatec pump). The typical vertical velocity associated to this flow is $1 \mu\text{m s}^{-1}$, which is significantly smaller than the other velocities involved in the experiment.

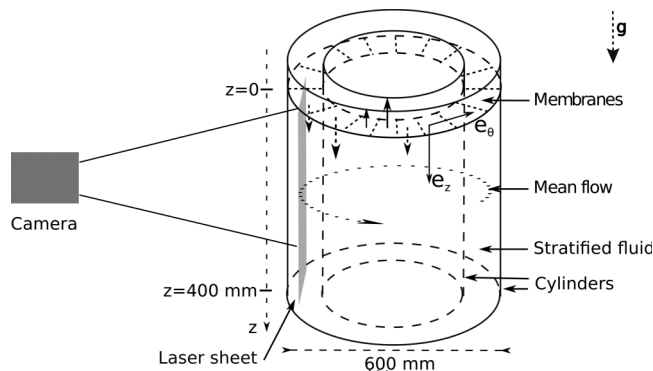


FIG. 1. Schematic view of the experimental setup.

The fluid is seeded with particles, whose density range is the same as the one of the fluid, so that particles can be found in the whole liquid at rest. Some of these particles are obtained by expanding nylon beads. The other beads are home-made by mixing alumina and paraffin wax. The particles are approximatively spherical and have a typical diameter of 0.5–2 mm. The characteristic time scale associated to the inertia of the beads is $t_0 = \rho_b d_b^2 / (18\eta_e)$, where ρ_b is the density of the bead, and d_b is its diameter. The maximal value of t_0 is about 0.2 s, which is much smaller than the periods of the waves (22–38 s): the Stokes number is small, and the particles actually follow the flow.

The particles at the center of the gap are illuminated using a laser sheet; the width of the selected plane is of about 30 mm. The particles are imaged in the whole height using a video camera (Allied Vision Stingray). Movies of typically 300 images are acquired at 3 frames per second every 100 s or 250 s. We have checked the influence of the position of the laser sheet by placing it closer to the wall (20 mm from the external wall instead of 60 mm when the laser is centered). The amplitudes of the wave and mean flow change by at most 25% when compared to the case where it is centered (data not shown). The value of the velocity thus depends only weakly on the transverse coordinate.

The velocity field is computed by particle image velocimetry (PIV) using OpenPIV software²⁰ (see the [supplementary material](#) for an example of a velocity field). The typical size of the interrogation windows is 32×32 pixels (corresponding to 11 mm). In each interrogation window, the velocity as a function of time is fitted using a sine function to obtain the amplitude and the phase of the wave (oscillation at the forcing angular frequency ω) and the mean flow. Some results are obtained using a fast Fourier transform of the same data (velocity as a function of time) on an integer number of periods (see the [supplementary material](#) for an example of a spectrum). The two procedures give similar results for the wave and the mean flow. The displayed values are averages over all the interrogation windows located at the same height, and for the values in the steady state averages on 5 successive movies. We do not apply any spatial filter before the averaging. We only analyze here the horizontal velocity $u(t)$ because it is significantly higher than the vertical one $v(t)$ so that its value is more accurately measured. For clarity, error bars are not displayed in the figures. The typical error in the mean flow and wave amplitude is 10%, estimated by comparing the values for several movies in the permanent regime.

The camera, the pump, and the motors are computer controlled using Labview routines.

III. MODEL

In this section, we present a two-dimensional model of the flow. This model neglects the curvature effect and the radial dependency: we consider a flow in a x, z plane, z being the downwards vertical direction and x corresponding to the θ direction as shown in Figure 1. The domain is periodic in the x direction. The model has been proposed by Plumb and McEwan.^{16,21}

We write the velocity \mathbf{V} as the sum of a mean velocity $\bar{\mathbf{V}}$ (average in the horizontal x direction in the model, average on a period in the experiments) and the fluctuation \mathbf{V}' : $\mathbf{V} = \bar{\mathbf{V}} + \mathbf{V}'$, with $\bar{\mathbf{V}} = \bar{u}\mathbf{e}_x$ and $\mathbf{V}' = u'\mathbf{e}_x + v'\mathbf{e}_z$ (\mathbf{e}_x is the unit vector in the x direction). In this model, the fluctuation is assumed to be the internal gravity wave at angular frequency ω : we neglect higher harmonics in this simple approach; in the experiment there are observed but are smaller than the wave amplitude (see the [supplementary material](#)).

The momentum equation for the mean flow writes

$$\frac{\partial \bar{u}}{\partial t} = -\frac{\partial F}{\partial z} + \nu \frac{\partial^2 \bar{u}}{\partial z^2} - \gamma \bar{u}, \quad (1)$$

where ν is the kinematic viscosity of the fluid, $F = \overline{u'v'}$ the wave momentum flux, and γ a decay rate which models the friction on the cylinders. Equation (1) is obtained from the Navier-Stokes equation by taking into account that the mean velocity is directed along the x direction: $\bar{\mathbf{V}} = \bar{u}\mathbf{e}_x$. Because of the periodic boundary condition, there is no mean pressure gradient here in contrast to the general case.²²

From the Navier-Stokes equation, the mass conservation, and incompressibility equation, one obtains using the Boussinesq and WKB approximations,¹⁶

$$F(\xi) = F(0) \times \exp \left(- \int_0^\xi \left[\frac{\alpha}{(1-U)^2} + \frac{1-\alpha}{(1-U)^4} \right] d\xi \right), \quad (2)$$

with

$$\begin{aligned} c &= \frac{\omega}{k_x}, \\ d &= \left(\frac{N\gamma}{k_x c^2} + \frac{N^3 \nu}{k_x c^4} \right)^{-1}, \\ \xi &= \frac{z}{d}, \\ U &= \frac{\bar{u}}{c}, \\ \alpha &= \frac{N\gamma d}{k_x c^2}, \end{aligned} \quad (3)$$

where k_x is the wave vector component in the x direction, c the phase velocity in the x direction, d the vertical dissipation length of the wave when there is no mean flow, and ξ the rescaled vertical coordinate. The denominators $(1-U)^2$ and $(1-U)^4$ in Equation (2) represent the feedback of the mean flow on the wave: the wave decay length is smaller when a mean flow has the same direction as the phase velocity of the wave in the x direction, which is the case in our experiments. All parameters of the previous equations are determined independently of the flow; the measure of γ is reported in Subsection 1 of the Appendix. In the present experiment, $|\bar{u}| < c$ so that there is no critical level.

To compare this model to the experimental data, we solve Equations (1) and (2) numerically. The only free parameter is $F(0)$. We obtain $F(\xi)$ using (2) and the experimental value of U . We integrate (1) with this value of $F(\xi)$ in the stationary regime, with the boundary conditions $\bar{u}(0) = 0$ and $\bar{u}(z_e) = 0$, where $z = 0$ correspond to the localization of the forcing and z_e is the bottom of the cell in the experiment. Taking $\bar{u}(0) = 0$ as a boundary condition is not obvious since the center of the membrane is moving and does not remain located at $z = 0$. The parameter $F(0)$ is determined by the best fit with the experimental data. The prediction for the horizontal wave component u' is obtained from the fit using the equation $F_{\text{fit}} = \frac{1}{2}(u')^2 \tan \theta$. This equation is obtained using the definition of θ , which is the angle between the vertical and the direction of the wavevector, and the orthogonality between the velocity and the wavevector. This angle is computed using the dispersion relation $\sin \theta = \omega/N$. The horizontal wave component u' is thus compared without any (new) fitting parameter to the experimental value.

IV. RESULTS

A. Dependence of the wave and mean flow on the forcing amplitude

We investigate in this section the dependence of the wave and the mean flow on the forcing amplitude M . An example of a raw velocity field and further explanations about the Fourier transform which is used to compute this wave amplitude and mean flow are given in the [supplementary material](#). The fact that the component oscillating at the forcing frequency has a progressive wave structure is checked in Subsection 2 of the Appendix.

The Fourier components of the horizontal velocity as a function of the forcing amplitude M in the steady state are displayed in Figure 2. We have checked that no peak exists at a subharmonic frequency by analysing long movies (25 forcing periods). The velocity is measured at height $z = 64$ mm. We observe that the amplitude of the horizontal wave component u' increases linearly with the forcing until $M = 4$ mm and then saturates. The amplitude of the mean flow \bar{u} increases quadratically with the forcing until the same value $M = 4$ mm. For larger forcing amplitude, the mean flow is larger than the wave which generates it. These behaviors are similar to the ones

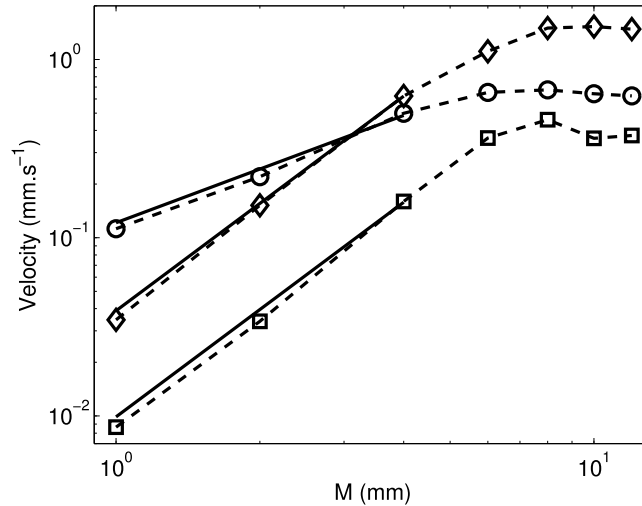


FIG. 2. Amplitude of the Fourier components of the horizontal velocity as a function of M in the steady state. Height $z = 64$ mm, $T = 38$ s, i.e., $\omega = 0.165$ rad s^{-1} , and $N = 1.44$ rad s^{-1} . $--\diamond$: mean flow \bar{u} , $--\circ$: horizontal wave component u' , and $--\square$: 2nd harmonic. The solid lines are a linear fit for the wave component, and quadratic fits for the mean flow and the 2nd harmonic.

observed in another geometry by King *et al.*⁶ Other harmonics are generated, and the 2nd harmonic has an amplitude of about the half of the wave amplitude for $M \geq 8$ mm. Significant 2nd harmonic amplitudes have been reported in another geometry.⁶ Results on the higher harmonics, which are always much smaller than the second one, are given in the [supplementary material](#).

In order to directly verify the link between the wave amplitude u' and the mean flow \bar{u} , we plot \bar{u} as a function of u' (see Figure 3). The mean flow is quadratic in the wave amplitude at small M . Both the mean flow and the wave saturate at high M . This is consistent with the results of Figure 2. The behavior of the Fourier components averaged in height is similar to the one at a given height (see the [supplementary material](#)).

We have shown that a mean flow is generated when a wave is forced. To ensure that a wave is necessary to observe a mean flow, we have performed experiments where $\omega > N$ ($T = 3$ s) so

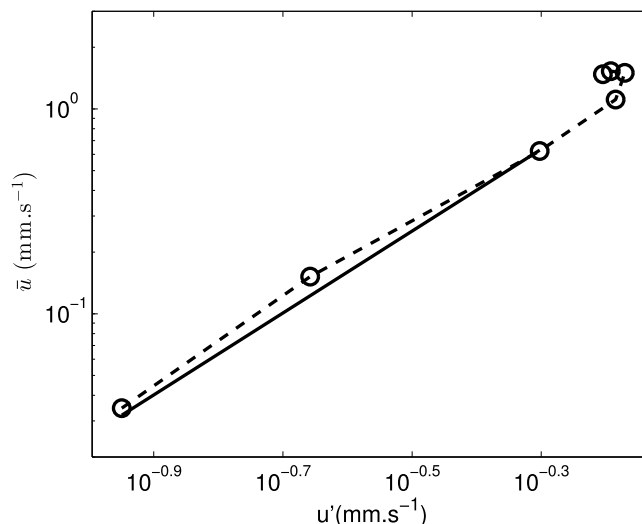


FIG. 3. Mean flow \bar{u} as a function of the horizontal wave component u' in the steady state. Height $z = 64$ mm, $T = 38$ s, and $N = 1.44$ rad s^{-1} . $--\circ$: experimental data and $--$: quadratic fit.

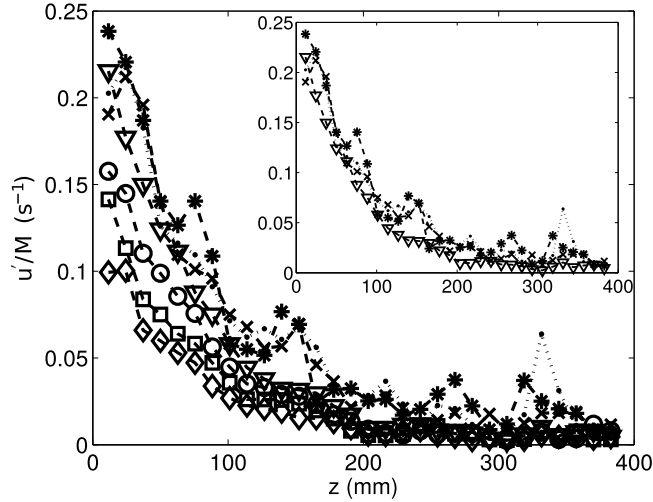


FIG. 4. Amplitude of the horizontal wave component u' normalized by the forcing amplitude M , as a function of height z . Steady state, forcing period $T = 38$ s, Brunt–Väisälä frequency: $N = 1.44$ rad s^{-1} . $\cdot\cdot\bullet$: $M = 1$ mm, $--\times$: $M = 2$ mm, $--*$: $M = 4$ mm, $--\nabla$: $M = 6$ mm, $--\circ$: $M = 8$ mm, $--\square$: $M = 10$ mm, and $--\diamond$: $M = 12$ mm. Inset: same curves, for $M \leq 6$ mm only.

that no wave can propagate in the fluid (data not shown). In that case no mean flow is generated as expected.

We have determined the dependence of u' and \bar{u} on the forcing amplitude M at a given altitude. In the following, we investigate this dependence on the whole height. The horizontal wave component normalized by the forcing amplitude M as a function of z is displayed in Figure 4. The amplitude of the wave decreases with z , i.e., when the measuring point is farther away from the membrane. This is due to the damping of the internal gravity wave by viscosity and wall friction. The values of u'/M decrease smoothly when M increases. The curves for $M \leq 6$ mm almost collapse on a master curve. The difference between this master curve and the curves for higher M is larger than the difference between the curves for $M \leq 6$ mm. This shows that u' is proportional to M everywhere for low forcing amplitude, up to roughly $M = 6$ mm. This confirms the conclusion of Figure 2 that the wave amplitude is proportional to M for low forcing amplitudes.

The amplitude of the mean flow normalized by M^2 is shown in Figure 5. The mean flow first increases and then decreases when z increases: this results from the competition between the no-slip boundary condition $\bar{u}(z = 0) = 0$ and localization close to the membrane of the forcing of the mean flow by the wave.

The curves for $M = 2, 4$, and 6 mm collapse on a master curve, showing that the mean flow is actually proportional to M^2 in that regime. The mean flow measured for $M = 1$ mm is very small so that the relative errors are large and this curve is only qualitative. When the forcing amplitude is larger, i.e., $M = 8, 10$, and 12 mm, the normalized mean flow decreases with M , which is consistent with the saturation shown in Figure 2.

In this section, we have shown that even at low forcing amplitude a mean flow is generated. For the small values of the forcing, i.e., $M \leq 4$ mm, the wave amplitude u' is proportional to the forcing and the mean flow is proportional to the square of the forcing in the steady state. For larger forcing amplitudes, the wave and mean flow almost saturate. In both regimes the mean flow is proportional to the square of the wave amplitude, which is consistent with Equation (1). We will see in Section IV C that the saturation of the wave amplitude is at least partially due to the feedback of the wave on the mean flow. With similar arguments we show in Figure 16 (the Appendix) that the saturation at high amplitudes cannot be explained only by a less efficient wave generation by the membrane.

In Secs. IV B–IV C, we discuss separately the two regimes: linear at small M and nonlinear at high M .

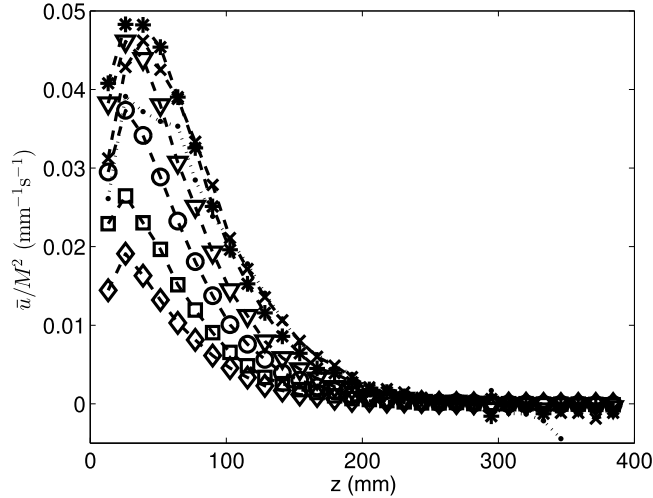


FIG. 5. Amplitude of the mean flow \bar{u} normalized by M^2 , as a function of height z . The amplitude is measured in the steady state. Forcing period $T = 38$ s, Brunt-Väisälä frequency: $N = 1.44$ rad s^{-1} . $\bullet\bullet$: $M = 1$ mm, $--\times$: $M = 2$ mm, $\cdot\cdot\times$: $M = 2$ mm, $--*$: $M = 4$ mm, $--\nabla$: $M = 6$ mm, $--\circ$: $M = 8$ mm, $--\square$: $M = 10$ mm, and $--\diamond$: $M = 12$ mm.

B. Generation of a mean flow without feedback on the wave

In this section, we study the case of low amplitude forcing, where the wave amplitude is increasing linearly with the forcing and where the mean flow is much lower than the horizontal wave phase velocity c . We will verify that the feedback of the mean flow on the wave is then negligible.

The amplitude of the horizontal wave component as a function of height for different times is shown in Figure 6(a). The initial time $t = 0$ corresponds to the beginning of the forcing. The data correspond to a small forcing amplitude: $M = 2$ mm. The wave amplitude is constant in time for $t \geq 150$ s, which is the time required to establish the wave in the whole cell.

The amplitude of the mean flow as a function of height for different times is shown in Figure 7(a). At every height, the mean flow increases with time until it reaches a constant value. The region where the mean flow is non-zero grows towards the bottom of the cell. The time scale of the growth of the mean flow is of the order of magnitude of γ^{-1} , the inverse of the decay rate due to the friction on the wall ($\gamma^{-1} \simeq 10^3$ s, see Subsection 1 of the Appendix). It is significantly larger

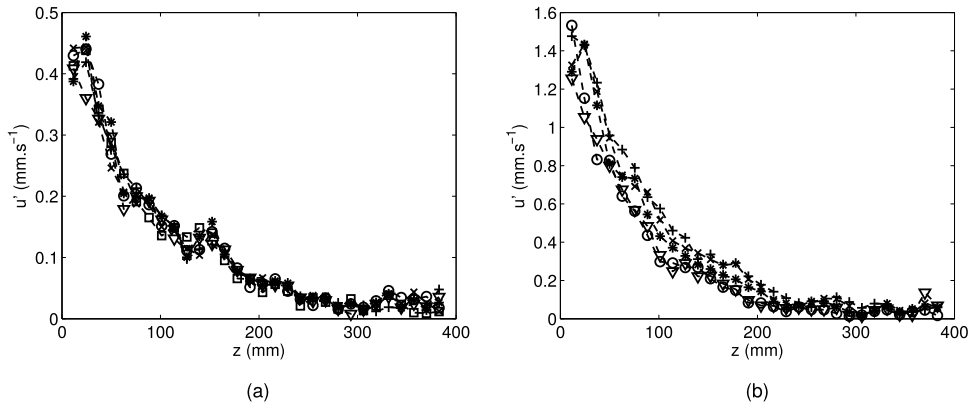


FIG. 6. Amplitude of the horizontal wave component u' as a function of height z at different times (time $t = 0$ corresponds to the beginning of the forcing), $T = 38$ s, $N = 1.44$ rad s^{-1} . (a) Low forcing amplitude $M = 2$ mm, times: $+$: $t = 150$ s, \times : $t = 350$ s, $*$: $t = 650$ s, ∇ : $t = 1050$ s, \circ : $t = 2050$ s, and \square : $t = 3050$ s. (b) Large forcing amplitude $M = 8$ mm, $T = 38$ s, $N = 1.44$ rad s^{-1} . Times: $+$: $t = 150$ s, \times : $t = 250$ s, $*$: $t = 450$ s, ∇ : $t = 2150$ s, and \circ : $t = 3250$ s.

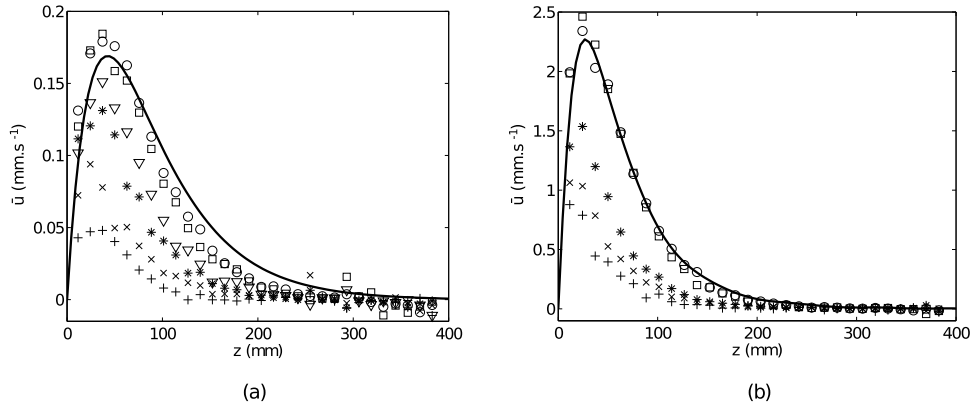


FIG. 7. Amplitude of the mean flow \bar{u} as a function of height z at different times, $T = 38$ s, $N = 1.44$ rad s^{-1} . (a) Low forcing amplitude $M = 2$ mm. Times: +: $t = 150$ s, \times : $t = 350$ s, $*$: $t = 650$ s, ∇ : $t = 1050$ s, \square : $t = 2050$ s, \circ : $t = 3050$ s, and $-$: fit with the model assuming a steady state regime. (b) Large forcing amplitude $M = 8$ mm. Times: +: $t = 150$ s, \times : $t = 250$ s, $*$: $t = 450$ s, \square : $t = 2150$ s, \circ : $t = 3250$ s, and $-$: fit with the model assuming a steady state regime.

than the time scale of the wave growth, which is of a few wave periods. The mean flow first appears close to the forcing membranes, where the wave amplitude is the larger (see Figure 6(a)), in qualitative agreement with Equation (1) describing the generation of the mean flow by the waves.

We now compare quantitatively the experimental data in the steady state with the model presented in Section III. The fit of the measured mean flow profile with the model is displayed in Figure 7(a). There is a single fitting parameter, which is $F(0)$, the flux at $z = 0$. The experimental data in the steady state regime (square and circle symbols) are well-fitted by the model, which assumes that the steady state regime has been reached. This shows that the generation of the mean flow can actually be described by the model of Section III.

The magnitude of the terms of Equation (1) which balance the forcing of the wave is displayed in Figure 8. This figure shows that none of these two terms is negligible: $\nu(\partial^2\bar{u})/(\partial z^2)$ is dominant at small z where the gradients of the wave amplitude are large and $-\gamma\bar{u}$ is dominant at larger z .

The experimental value of the wave u' is compared in Figure 9(a) to the value deduced from the fit of the mean flow (Figure 7(a)), without any new fitting parameter. The experimental data are in qualitative agreement with the result from the fit and display a similar trend. The origin of

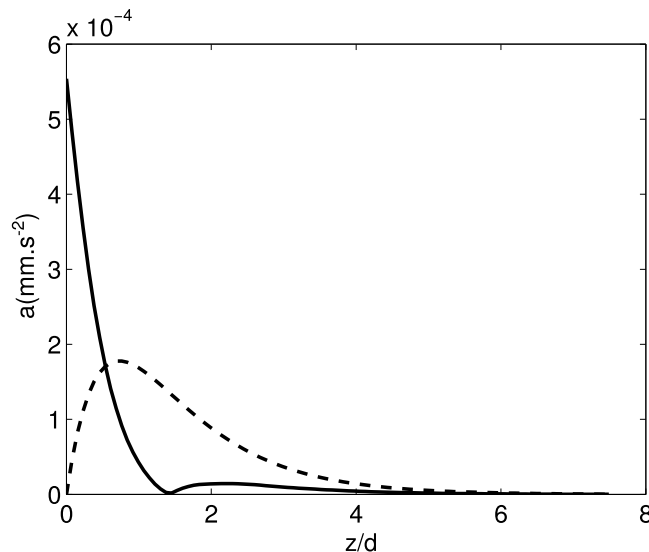


FIG. 8. Value of the two terms of the model in the calculation of the fit of Figure 7(a). $---$: $\gamma\bar{u}$ and $-$: $|\nu\partial^2\bar{u}/(\partial^2z)|$.

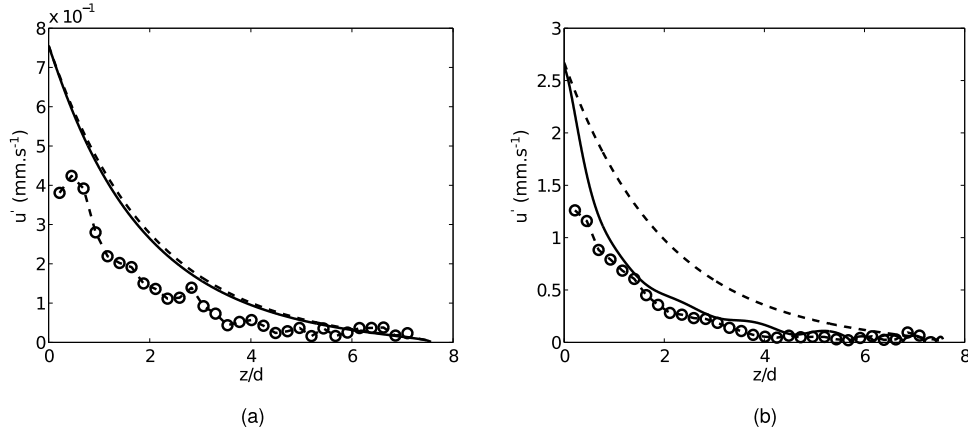


FIG. 9. Comparison of the experimental wave amplitude and the value deduced from the fit, $T = 38$ s, $N = 1.44$ rad s $^{-1}$. $-\circ-$: experimental data, $-$: value from fit, and $--$: value computed from flux with same value at $z = 0$ but without taking into account the feedback of the mean flow on the wave for the decay, i.e., with $U = 0$ in Equation (2). (a) Low forcing amplitude $M = 2$ mm. (b) Large forcing amplitude $M = 8$ mm.

the discrepancy is not clear. It may be due to differences between the hypotheses of the model and the experiment; for example, in the experiment the velocity is not perfectly constant in the radial direction. For this experiment, the damping taking into account the feedback of the mean flow on the wave is almost the same as the one without any feedback. The model thus predicts a negligible feedback, as observed experimentally.

The ratio of the viscous damping in the bulk to the wall friction term in the expression of d , which is equal to $(1 - \alpha)/\alpha$ (see Equation (3)), is about 20. For this experiment, the value of d is mostly due to the viscous damping in the bulk. The limit angular frequency ω_l for which these two terms are equal is $\omega_l = \nu^{1/2} N k_x / \gamma^{1/2}$, which corresponds to a period $T = 8$ s: even when changing the frequency (see Section IV D), the damping by wall friction is negligible for the waves in the present experiment. On the contrary, both the viscous damping in the bulk and the friction on the walls affect the value of the mean flow (see Figure 8).

C. Generation of a mean flow with feedback on the wave

We now consider a higher wave amplitude, where the mean flow is comparable to the horizontal wave phase velocity c . We will observe that the feedback of the mean flow on the wave is then significant.

The horizontal wave component as a function of height for different times is displayed in Figure 6(b). The forcing amplitude is large: $M = 8$ mm. The wave velocity decreases when z increases, i.e., when the distance to the forcing membrane increases. The wave amplitude is decreasing with time, especially between $z \sim 50$ mm and $z \sim 200$ mm. This is in contrast with the case of low forcing amplitudes (see Figure 6(a)).

The mean flow as a function of height, for different times, is shown in Figure 7(b). As in the low forcing amplitude limit (see Figure 7(a)), the mean flow is generated first at the top of the cell, and then the region where the mean flow is present grows towards the bottom of the cell.

The decrease of the wave amplitude is correlated with the increase of the mean flow amplitude (see Figures 6(b) and 7(b)). The mean flow amplitude is here high enough to lower the wave amplitude in the steady state: there is a negative feedback of the mean flow on the wave. The ratio \bar{u}/c is close to 0.25, so that a significant feedback is actually expected from Equation (2).

The fit of the experimental mean flow with the model is shown in Figure 7(b). The agreement is good when the steady state is reached, which is an assumption of the model. This agreement is not obvious because the model does not take into account higher harmonics which are well developed at large forcing (see Figure 2 where harmonics 2 is shown).

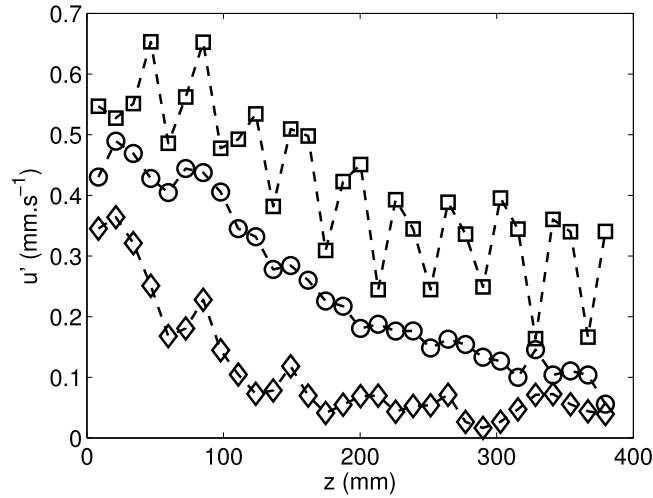


FIG. 10. Wave amplitudes as a function of forcing frequency. $M = 2$ mm and $N = 1.46 - 1.52$ rad s^{-1} . $--\diamond$: $T = 38$ s, i.e., $\omega = 0.165$ rad s^{-1} , $--\circ$: $T = 28$ s, i.e., $\omega = 0.224$ rad s^{-1} , and $--\square$: $T = 22$ s, i.e., $\omega = 0.286$ rad s^{-1} .

The experimental values of the wave amplitude and the value deduced from the fit are displayed in Figure 9(b). The agreement between the two curves is fair, showing that the model correctly describes the generation of the mean flow by the wave even in the case where the mean flow retroacts on the wave. This feedback is taken into account in the model but higher harmonics are not. The difference between the curves in plain line (feedback taken into account) and dashed line (no feedback) is large. The model thus predicts a large feedback, as observed experimentally.

D. Effect of the forcing frequency

The previous results have been obtained for a forcing period $T = 38$ s. In this section we investigate the effect of the forcing frequency on the mean flow generation. The amplitude is kept constant at $M = 2$ mm; similar results are obtained for other amplitudes.

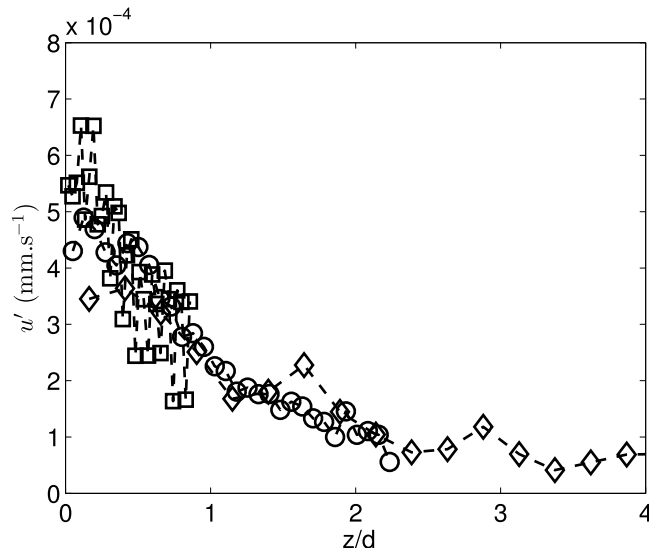


FIG. 11. Experimental wave amplitudes as a function of z/d . Steady state $M = 2$ mm and $N = 1.46 - 1.52$ rad s^{-1} . $--\diamond$: $T = 38$ s, $--\circ$: $T = 28$ s, and $--\square$: $T = 22$ s.

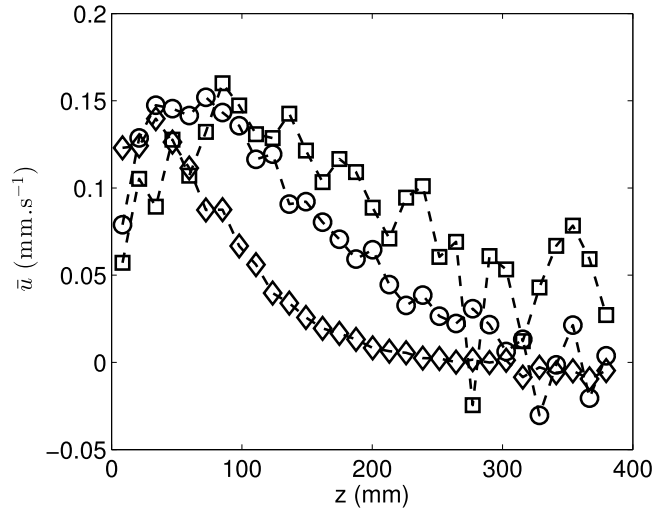


FIG. 12. Mean flow at different forcing frequencies. Steady state $M = 2$ mm and $N = 1.46 - 1.52$ rad s^{-1} . $--\diamond$: $T = 38$ s, $--\circ$: $T = 28$ s, and $--\square$: $T = 22$ s.

In Figure 10 we display the variation of the horizontal component of the wave u' as a function of height for different forcing periods. The typical length of variation of u' increases when T decreases. For $T = 22$ s, u' does not vanish at the bottom of the cell ($z \approx 400$ mm). There is some reflection at the bottom of the cell,²³ which explains the modulation of u' (see the [supplementary material](#)).

The same experimental data with z normalized by d are shown in Figure 11. The experimental curves collapse on the same master curve. This rescaling as a function of z/d confirms the prediction of Equation (2). The independence of $u'(z = 0)$ with ω can be understood by a scaling argument. If ε is the vertical displacement of the membrane, the vertical wave velocity verifies $v' \propto \omega \varepsilon$. As a consequence of the dispersion relation, the horizontal wave component verifies $u' = v' / \tan \theta$, and for small θ : $\tan \theta \approx \sin \theta = \omega / N$. Note that this scaling argument is in agreement with the calculation of Plumb and McEwan¹⁶ where $F = \overline{v'u'}$ is proportional to ω .

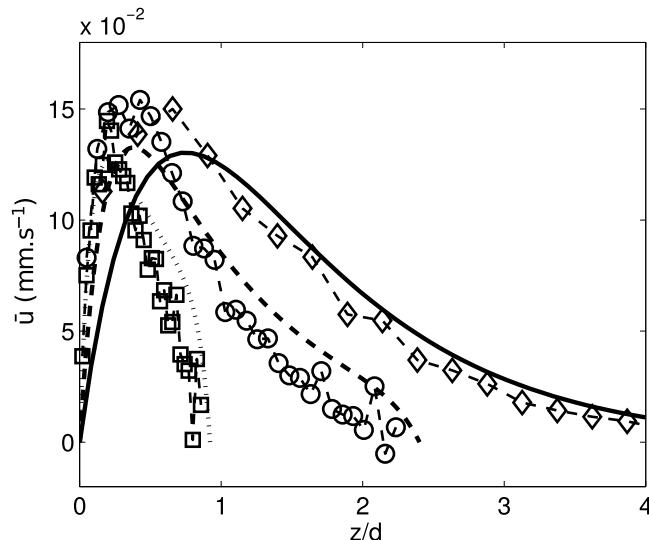


FIG. 13. Mean Flow. Steady state $M = 2$ mm and $N = 1.46 - 1.52$ rad s^{-1} . $--\diamond$: experimental data $T = 38$ s, $-$: fit, $--\circ$: experimental data $T = 28$ s, $-$: fit, $--\square$: experimental data $T = 22$ s, and $-$: fit.

The dependence of the mean flow with height for several forcing periods is displayed in Figure 12. The width of the mean flow curve is larger when the period decreases. This is consistent with the fact that the wave has a large value on a larger width. The link is however not simple. In Figure 13 we show the same experimental data with z normalized by d . The fits show that the model is suitable to describe these data. The curves do not collapse on a single master curve because the mean flow is not only saturated by the term $-\gamma\bar{u}$, but also by the term $\nu(\partial^2\bar{u})/(\partial z^2)$. The latter term is large at large values of T , because the wave is strongly localized.

In conclusion, the main effect of a frequency change on the wave is linked to a change of the vertical dissipation length d . The mean flow is localized on a larger height if T decreases; the curves do not collapse on a master curve when normalizing z by d because in the equation determining the mean flow two terms containing this mean flow balance the forcing by the wave.

V. CONCLUSION

We have studied experimentally the generation of a mean flow by a progressive internal gravity wave in a simple 2D geometry, i.e., for a stratified fluid located between two cylinders. In this geometry, because of the periodicity in the azimuthal direction, a large azimuthal mean flow is possible as it is only slightly damped.

At small forcing, the wave amplitude is linear in the forcing amplitude and the mean flow is quadratic. The mean flow is thus quadratic in the wave amplitude, which is consistent with the quadratic non-linear term of the Navier-Stokes equation. At higher forcing the wave and the mean flow saturate, at least partly due to the feedback of the mean flow on the wave. The forcing of higher harmonics may also be involved in this saturation.

At low wave amplitude, the mean flow is much smaller than the wave horizontal phase velocity c , and there is no feedback of the mean flow on the wave. On the contrary, at large wave amplitude, the mean flow is comparable to the wave horizontal phase velocity c . The mean flow remains smaller than c , i.e., there is no critical level in this experiment. As expected from the model, there is a feedback of the mean flow on the wave. The mean flow tends to decrease the amplitude of the wave, i.e., the feedback is negative.

The experimental results can be explained using a 2D analytical model. This model assumes that the wave is propagating downwards and is mainly damped by bulk viscosity. Because of momentum equation, a mean flow is induced by the wave. The retroaction of the mean flow on the wave is obtained using the Navier-Stokes equation, mass conservation, and WKB and Boussinesq approximations.

When decreasing the period of the wave, the wave is damped on a larger distance and the mean flow is located farther away from the forcing membrane. The behavior of the wave is due to a change of the dissipation length d (at least as long as the feedback on the wave is not too large), which can be calculated from the experimental parameters. The variation of the shape of the mean flow is also in agreement with the model.

The next step will be to investigate other forcings, such as the case of a stationary wave in the azimuthal direction, to reproduce the quasi-biennial oscillation and characterize the generation of the mean flow by two counter-propagating waves, and the feedback of the mean flow on these waves.

SUPPLEMENTARY MATERIAL

See [supplementary material](#) for additional figures and discussions, in particular, about the data analysis.

ACKNOWLEDGMENTS

We gratefully acknowledge N. Garroum, J. da Silva Quintas, C. Goncalves, E. Nicolau, C. Herrmann, and L. Bonnet for their technical support. We thank Alexandre Paci for discussions and

for providing us with nylon beads. This work has been supported by the Agence nationale de la recherche (Grant No. ANR-12-BS04-0005). The experiments have been performed in the laboratory of the Institut de physique du globe de Paris located at Saint-Maur-des-Fossés.

APPENDIX: ADDITIONAL MEASUREMENTS

1. Decay of mean flow

The decay of the mean flow is displayed in Figure 14. This decay is measured after switching off the forcing. It is mostly due to the friction on the walls, but also takes into account the small friction on the membranes. The measurements are obtained using a tracking algorithm, which gives similar results as PIV for this flow. The value of the mean flow is here the value averaged in height. This value decreases exponentially with time, and the decay rate is independent of the initial value of the mean flow. This allows us to define a decay rate $\gamma \sim 10^{-3} \text{ s}^{-1}$ for the mean flow. This value is close to the one found by Plumb and McEwan.¹⁶

2. Profile of the wave

The phase φ_0 at initial time is obtained by fitting the horizontal velocity with a sine function of angular frequency ω . The corresponding isolines are shown in Figure 15. The dependence of this phase on height, in bands slightly inclined from the horizontal, shows that a progressive wave is actually generated. The dependence of the phase in the x direction at a given height is consistent with the expected value (400 mm, set by the curvilinear distance between 4 motors), and the wavelength in the z direction is consistent with this value and the dispersion relation (a vertical wavelength of 61 mm is expected here).

3. Comparison of the wave amplitude initially and in steady state

We compare in Figure 16 the wave amplitude just after starting the forcing (time 100–200 s) and in the steady state. There is no difference for the smaller forcing amplitudes, because the wave is not affected by the mean flow. In the steady state, the wave amplitude remains linear until $M = 6$ mm. The wave amplitude is always smaller than its initial value. Since the major change

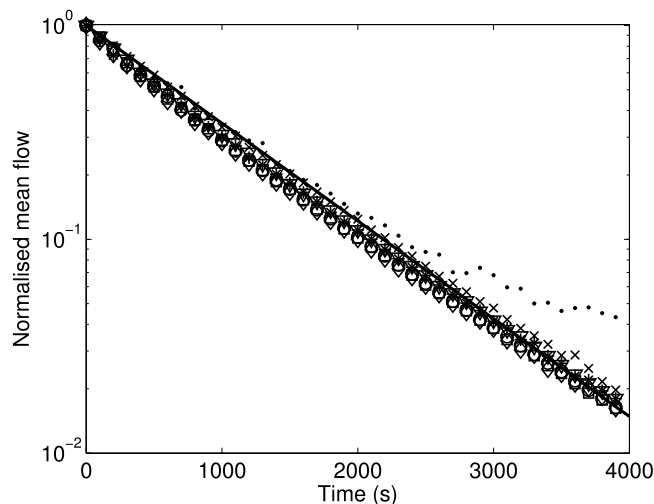


FIG. 14. Decay of the mean flow as a function of time, when the forcing is switched off. The mean flow is rescaled by its value at $t = 0$, which is here the time when the forcing is stopped. $T = 38$ s and $N \in [1.45 - 1.4] \text{ s}^{-1}$. Forcing amplitude before the forcing is stopped: $\bullet\bullet$: $M = 1$ mm, $--\times$: $M = 2$ mm, $\cdot\cdot\times$: $M = 2$ mm, $--*$: $M = 4$ mm, $--\nabla$: $M = 6$ mm, $--\circ$: $M = 8$ mm, $--\square$: $M = 10$ mm, and $--\diamond$: $M = 12$ mm. Solid line: fit with $\exp(-t/\tau)$, with $\tau = 950$ s.

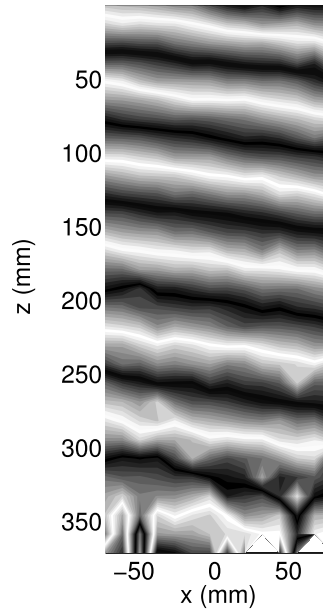


FIG. 15. Phase of the wave component (component at ω). $T = 28$ s, $M = 8$ mm, and $N = 1.49$ rad s^{-1} . Black: $\varphi_0 = 0$ and white: $\varphi_0 = \pi$.

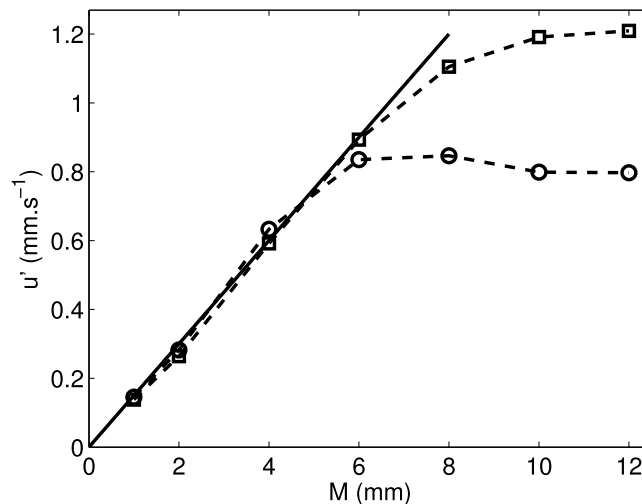


FIG. 16. Comparison of the horizontal wave amplitude as a function of the forcing, 100–200 s after the beginning of the forcing ($--\square$) and in the steady state ($--\circ$). $-$: linear fit. Height $z = 64$ mm, $T = 38$ s, and $N = 1.44$ rad s^{-1} .

between the initial and steady state is that the mean flow increases (the amplitudes of the harmonics are almost constant), this variation is due to the feedback of the mean flow on the wave. The initial wave amplitude remains linear until $M = 8$ mm only. The saturation at “initial” time may be due to the very fast generation of a mean flow, at the time scale of a few periods, when the forcing is high, or to the injection of power in harmonics, which in turn reduces the power available for the wave.

¹ J. Lighthill, “Acoustic streaming,” *J. Sound Vib.* **61**, 391–418 (1978).

² O. Bühler, *Waves and Mean Flows* (Cambridge University Press, 2009).

³ M. S. Longuet-Higgins, “Longshore currents generated by obliquely incident sea waves, I,” *J. Geophys. Res.* **75**, 6778–6789, doi:10.1029/JC075i033p06778 (1970).

⁴ O. Bühler and T. E. Jacobson, “Wave-driven currents and vortex dynamics on barred beaches,” *J. Fluid. Mech.* **449**, 313–339 (2001).

- ⁵ M. Baldwin, L. Gray, T. Dunkerton, K. Hamilton, P. Haynes, J. Holton, M. Alexander, I. Hirota, T. Horinouchi, D. Jones, J. Kinnersley, C. Marquardt, K. Sato, and M. Takahashi, "The quasi-biennial oscillation," *Rev. Geophys.* **39**, 179–229, doi:10.1029/1999RG000073 (2001).
- ⁶ B. King, H. P. Zhang, and H. L. Swinney, "Tidal flow over three-dimensional topography in a stratified fluid," *Phys. Fluids* **21**, 116601 (2009).
- ⁷ X. Li and P. Read, "A mechanistic model of the quasi-quadrennial oscillation in Jupiter's stratosphere," *Planet. Space Sci.* **36**, 637–669 (2000).
- ⁸ T. Fouchet, S. Guerlet, D. F. Strobel, A. A. Simon-Miller, B. Bézard, and F. M. Flasar, "An equatorial oscillation in Saturn's middle atmosphere," *Nature* **453**, 200–202 (2008).
- ⁹ M. Yamamoto and M. Takahashi, "The fully developed superrotation simulated by a general circulation model of a Venus-like atmosphere," *J. Atmos. Sci.* **60**, 561–574 (2003).
- ¹⁰ F. Bretherton, "On the mean motion induced by internal gravity waves," *J. Fluid. Mech.* **36**, 785–803 (1969).
- ¹¹ T. S. van den Bremer and B. R. Sutherland, "The mean flow and long waves induced by two-dimensional internal gravity wavepackets," *Phys. Fluids* **26**, 106601 (2014).
- ¹² N. Wedi and P. Smolarkiewicz, "Direct numerical simulations of the Plumb-McEwan laboratory analog of the QBO," *J. Atmos. Sci.* **63**, 3226–3252 (2006).
- ¹³ N. Grisouard and O. Bühler, "Forcing of oceanic mean flows by dissipating internal tides," *J. Fluid. Mech.* **708**, 250–278 (2012).
- ¹⁴ G. Bordes, A. Venaille, S. Joubaud, P. Odier, and T. Dauxois, "Experimental observation of a strong mean flow induced by internal gravity waves," *Phys. Fluids* **24**, 086602 (2012).
- ¹⁵ T. Kataoka and T. R. Akylas, "On three-dimensional internal gravity wave beams and induced large-scale mean flows," *J. Fluid. Mech.* **769**, 621–634 (2015).
- ¹⁶ R. Plumb and A. McEwan, "The instability of a forced standing wave in a viscous stratified fluid: A laboratory analogue of the quasi-biennial oscillation," *J. Atmos. Sci.* **35**, 1827–1839 (1978).
- ¹⁷ N. Otobe, S. Sakai, S. Yoden, and M. Shiotani, "Visualization and WKB analysis of the internal gravity wave in the QBO experiment," *Nagare: Jpn. Soc. Fluid Mech.* **17** (1998); available at <http://www2.nagare.or.jp/mm/98/otobe/index.htm>.
- ¹⁸ L. Gostiaux, "Étude expérimentale des ondes de gravité internes en présence de topographie. Émission, propagation, réflexion," Ph.D. thesis, École Normale Supérieure de Lyon, 2006.
- ¹⁹ J. Kestin, H. Khalifa, and R. Correia, "Tables of the dynamic and kinematic viscosity of aqueous NaCl solutions in the temperature range 20–150 C and the pressure range 0.1–35 MPa," *J. Phys. Chem. Ref. Data* **10**, 71–87 (1981).
- ²⁰ Z. J. Taylor, R. Gurka, G. A. Kopp, and A. Liberzon, "Long-duration time-resolved PIV to study unsteady aerodynamics," *IEEE Trans. Instrum. Meas.* **59**, 3262–3269 (2010).
- ²¹ R. Plumb, "The interaction of two internal waves with the mean flow: Implications for the theory of the quasi-biennial oscillations," *J. Atmos. Sci.* **34**, 1847–1858 (1977).
- ²² J. Lighthill, *Waves in Fluids* (Cambridge University Press, 1980).
- ²³ M. Mercier, N. Garnier, and T. Dauxois, "Reflection and diffraction of internal waves analysed with the Hilbert transform," *Phys. Fluids* **20**, 086601 (2008).